JOURNAL OF MATERIALS SCIENCE **37** (2002) 1413–1420

The nature of Pr-$ZrSiO_4$ yellow ceramic pigment

J. A. BADENES, J. B.VICENT, M. LLUSAR, M. A. TENA, G. MONRÓS
Department of Inorganic and Organic Chemistry, Jaume I University, Castellón, Spain

Pr-$ZrSiO_4$ yellow ceramic pigment is believed to be a solid solution of Pr^{4+} with the zircon lattice, but studies are poor and scarce. The aim of this paper is the synthesis of Pr-$ZrSiO_4$ yellow pigment in the presence of NaF by several non-conventional methods and to investigate the nature of the pigment. Results indicate that the formation of Pr-$ZrSiO_4$ yellow pigment must be explained by two simultaneous mechanisms: formation of a solid solution of Pr in a $ZrSiO_4$ network and an occlusion mechanism.

1. Introduction

Throughout history various yellow ceramic pigments have been used: yellow of vanadium-zirconia, tin-vanadium yellow, cadmium yellows, lead antimoniate ($PbSbO_3$), etc. The praseodymium zircon yellow ceramic pigment arises from the need for a clean and bright yellow colour, characteristics lacking in the foregoing colours [1]. Its commercial preparation has been possible by progress in rare earth chemistry over the period 1950–1960 which allows the preparation of high purity praseodymium oxide.

In 1952 a zircon yellow pigment was obtained using didyum, a mixture of Nd and Pr. In 1956 this pigment was produced with rare earths and NaCl plus Na_2MoO_4 as mineralizer agent [2], showing that Pr was the chromophore agent (La, Ce turned the colour pale and Nd altered the tone of the colour).

Seabright patented the colour in 1961 [3]. The use of halides as mineralizers was initiated by Seabright [4] in order to obtain an intense pigment, although the intensity is limited (additions above 5% by weight Pr_6O_{11} do not improve the intensity).

Booth and Peel [5] presented an empirical study about the best experimental conditions: Pr_6O_{11} content increased the yellow tone, NaF content increased the intensity of the colour, equimolar mixtures of ZrO_2 and SiO_2 optimized the intensity and the best calcination temperature was between 1200–1300°C maintained for one hour.

Several studies have shown that for all zircon based colours, the doping ion must be present during formation of the zircon crystal by reaction of the constituent oxides [5–8]. Batchelor [9] claims that to produce a good pigment, three mineralizing ions are required: alkali, fluoride and another halide (chloride or bromide). The role played by mineralizers in the formation of the colour has been something of a mystery.

A partial explanation for the colouring mechanism has been found in the works of Eppler [10, 11] who applied the well-known "marker technique" [12, 13] for solid state reaction to this system: the two components SiO_2 and ZrO_2 were placed in layers and platinum wires were laid as markers at the interface. If there is counterionic movement and diffusion of Zr^{4+} and Si^{4+}, zircon will appear on both sides of the markers. If only one of the cations diffuses, the zircon will be formed only on the side of non-diffusing cation. Moreover, if vapour-phase diffusion is involved, the product not only appears at the interface but at all free surfaces, and it is found around the whole periphery on the non-diffusing cation. This is what occured in the vanadium-zircon system and praseodymium-zircon yellow system [11]: when vanadium or praseodymium compounds and mineralizer are equally dispersed in both phases, the silica layer remained white, but coloured zircon appeared at the interface on the side of the zirconia.

Hence, the mechanism is thought to be a reaction between SiO_2 and NaF to form volatile SiF_4:

$$SiO_2 + 4NaF \rightarrow SiF_4 + 2Na_2O$$

Now the silicon ions must be transported in some manner across the product layer to the interface with unreacted zirconia; Eppler postulates two alternatives for this: the ion diffusion model and the vapour transport model. The former assumes that silicon tetrahalides decompose on the surface of the product layer leaving the silicon in imperfections in the product layer. Silicon ions and the electrons can then diffuse through the product layer to the interface with zirconia layer where they react to form zircon [3]:

$$SiF_4 \rightarrow Si^{4+} + 4e^- + 2F_2$$

$$Si^{4+} + 4e^- + ZrO_2 + O_2 \rightarrow ZrSiO_4$$

The vapour transport pattern postulates that the silicon halides as well as the oxygen pass in the vapour state through pores in the product layer:

$$SiF_4 + ZrO_2 + O_2 \rightarrow ZrSiO_4 + 2F_2$$

The Eppler mechanism for the V-$ZrSiO_4$ and Pr-$ZrSiO_4$ pigments concludes that vanadium and

praseodymium compounds react with mineralizers and are transported to the reaction sites in the vapour state. On the contrary, in Fe-$ZrSiO_4$ pigment, the iron-zircon layer forms on the ZrO_2-side of the interface, but not round the periphery of the vessel, when iron and mineralizers are in both layers. This demonstrates the immobility of iron, compared with vanadium and praseodymium, explaining why the iron-pink is a more difficult colour to produce.

For the vanadium-zircon blue pigment it is assumed that a V-$ZrSiO_4$ solid solution exists [5, 14]. Some authors believe that iron-zircon pink is an inclusion pigment [15] but other authors doubt this suggestion [16]. Finally the Pr-$ZrSiO_4$ yellow pigment is traditionally believed to be a solid solution in a zircon lattice [5, 8] with Pr^{4+} (without excluding certain amount of Pr^{3+}) substituting for Zr at its dodecahedral position [17]. A recent work [18] is in agreement with the existence of a solid solution in V-$ZrSiO_4$ pigment, an inclusion pigment for iron-zircon pink and the mixed nature of Pr-$ZrSiO_4$ yellow pigment, but studies are poor and scarce on the origin of the yellow colour.

The aim of this paper is the synthesis of Pr-$ZrSiO_4$ yellow pigment in presence of NaF by several non-conventional methods and to investigate the nature of the pigment.

2. Experimental

A praseodymium-zircon yellow pigment with SiO_2.$0.90ZrO_2$.$0.05Pr_2O_3$.0.20NaF composition has been prepared by three different methods: ceramic method (CEF sample), colloidal gel route (CGF sample) and polymeric gel from alkoxides method (PGF sample). Alternative samples without NaF addition (CE, CG and PG samples), of SiO_2.$0.90ZrO_2$.$0.05Pr_2O_3$ composition have been studied in order to know the role played by halides in the colour preparation.

The precursors in ceramic method (CE) were: zirconia of industrial quality, quartz also of industrial quality and Pr_6O_{11} (from Rhone Poulenc). These precursors were mixed in a planetary ball mill for 20 minutes in acetone media.

In the colloidal gel method (CG), a solution containing $ZrOCl_2.8H_2O$ (MERCK), colloidal silica supplied for QUIMIDROGA and Pr_6O_{11} was obtained by dissolving the different precursors in water with continuous stirring at 70°C. When a homogeneous solution was reached, a concentrated aqueous solution of ammonia was added until gelation occurred at pH = 5–6. The light yellow and homogeneous gel obtained was aged and dried at room temperature in the open air, and then grinded in an agate mortar.

In the polymeric gel method (PG), the precursor of praseodymium (Pr_6O_{11} from Rhone Poulenc), was refluxed at 70°C for 45 minutes in ethanol media acidified with HNO_3. Then acetylacetone (from PANREAC) was added and refluxed 30 minutes under the same conditions until a solution was achieved. TEOS (from ALDRICH) was then added and prehydrolised for 2 hours. After that zirconium n-propoxide and NaF were dissolved in the refluxed media for 24 hours and geled in open air. The conditions of preparation of polymeric gels are summarized in Table I.

TABLE I Conditions of preparation of polymeric samples

	Molar ratio
$Zr(OPr)_4$:EtOH	1 : 26
$Zr(OPr)_4$:acac	1 : 1
$Zr(OPr)_4$:H_2O	1 : 3
$Zr(OPr)_4$:H^+	1 : 0.1

$Zr(OPr)_4$: zirconium n-propoxide;
acac: acetylacetone; EtOH: ethanol.

Samples were firs studied by DTA-TGA-DTGA (Differential Thermic, Thermogravimetric and Differential Thermogravimetric analysis). The analyses were carried out in a Perkin-Elmer analizer using a heating rate of 5°C/min up to 1150°C.

Raw samples were also characterized by IR (Infrared) spectroscopy. The IR studies were carried out in a Perkin-Elmer spectrophotometer between 200 and 2400 cm^{-1} by the conventional KBr tablet method.

In order to follow the different reaction mechanisms succesive thermal treatments with a relative long soaking time (12 hours) were performed at temperatures of 300, 600, 700, 800, 900, 1000, 1100, 1200, 1250 and 1300°C.

Fired samples were characterized by several methods: (a) XRD (X-Ray Diffraction) analysis was performed in a Philips PW1729 diffractometer using Ni filtered Cu K_α radiation. XRD analysis at relatively high goniometer speed was used in order to determine the crystalline phases present in the sample, and the technique was also used at low goniometer speed using fine α-Al_2O_3 as an internal standard in order to measure the evolution of zircon cell parameters by the POWCAL and LSQC calculation programmes [19]; (b) IR (Infrared) Spectroscopy was carried out under the same conditions mentioned above for raw samples; (c) UV-VIS-NIR (ultraviolet, visible and near infrared) spectroscopy using diffuse reflactance was performed in a Perkin-Elmer LAMBDA spectrophotometer. From these spectra CIE-$L^*a^*b^*$ colour measurements (L^* eclairage: $L = 0$ black to $L = 100$ white, a^*: green(−) → red (+) and b^*: blue (−) → yellow (+) axes) were determined [20]; (d) Microstructural analysis by SEM-EDX (Scanning Electron Microscope-Energy Dispersion X-Ray) was carried out in a LEICA LEO440I equiped with an Oxford LYNK EDX system.

3. Results and discussion

3.1. Previous characterization of raw samples: thermal analysis (DTA/TGA)

In order to have previous information about the behaviour of the samples during the firing treatment, a thermal characterization was performed on raw samples. The DTA-TG results obtained for CGF sample are depicted in Fig. 1. The CGF analysis indicates endothermic bands at 150°C (water evaporation) and 340°C (chloride volatilization), and a very weak exothermic band at 460°C, associated with tetragonal and monoclinic zirconia crystallization (detected by

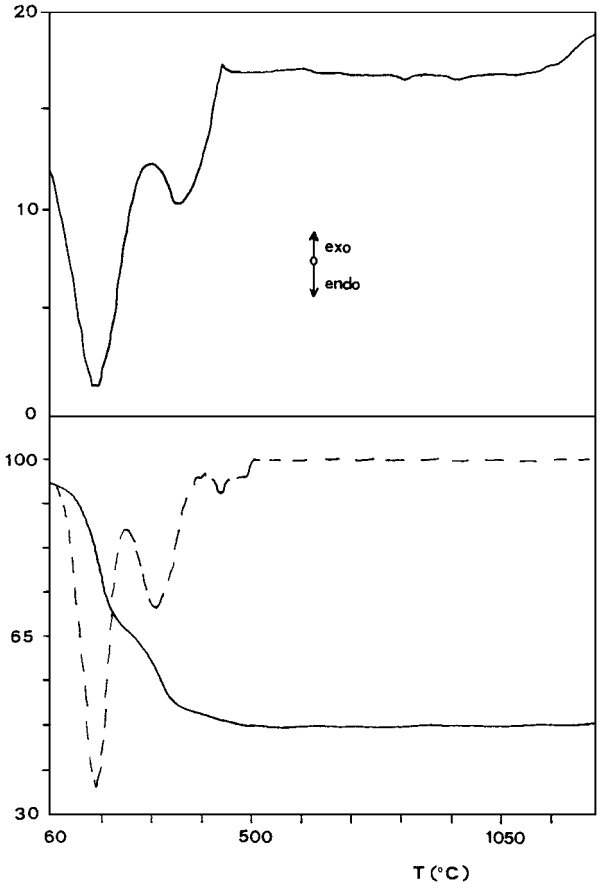

Figure 1 DTA-TG-DTG analysis of sample CGF.

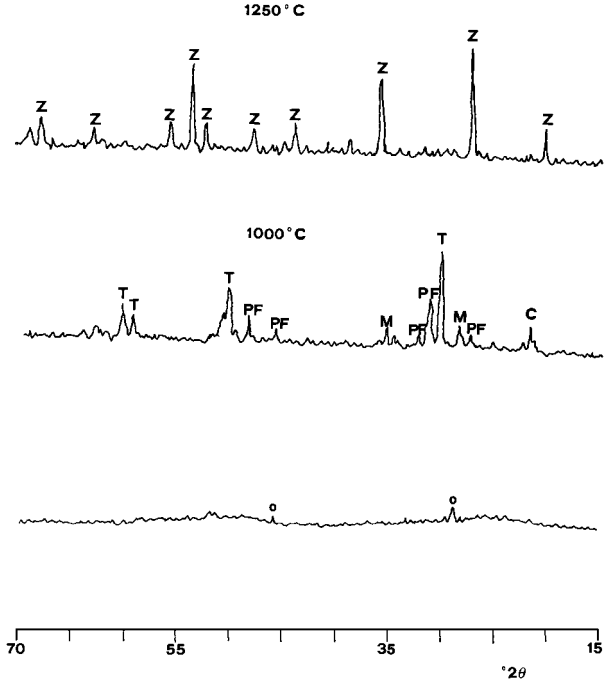

Figure 2 XRD patterns of PGF sample: raw, 1000 and 1250°C fired samples. O(Pr_6O_{11}), Z($ZrSiO_4$), T(t-ZrO_2), PF(Na_2 $Pr_8(SiO_4)_6F_2$), C(Cristobalite), M(m-ZrO_2).

XRD in residual samples). TG-DTG analysis indicated a mass loss at 150°C and 340°C associated with humidity and chloride elimination, respectively. In CEF sample, an additional exothermic band is detected at 840°C associated with zircon crystallization (detected by XRD together with quartz and monoclinic zirconia in the residual sample). In the polymeric gel samples, besides the water evaporation band centered at 140°C, two strong exothermic bands are detected at 280°C and 370°C, associated with organic combustion, and one exothermic weak band at 400°C, assigned to tetragonal zirconia crystallization (the only crystalline phase detected by XRD of the DTA-TG residue).

3.2. X-Ray difraction (XRD) characterisation

XRD results obtained and the evolution of the colour with temperature of samples are shown in Table II. The evolution of XRD for PGF sample is presented in Fig. 2.

The CE sample remained gray all over the thermal treatment, and only above 1250°C is the zircon detected. The addition of NaF (CEF), diminished the zircon temperature detection to 1100°C. However, two results are notable: (a) the appearance of yellow colour in CEF is associated with zircon crystallization, and (b) at 700°C the $Na_2Pr_8(SiO_4)_6F_2$ (yellow-green colour according to US ASTM card 20-1151) crystalline phase is detected and remains in the overall treatment.

In the colloidal gel sample without fluorides (CG), the initial NH_4Cl detected disappears at 300°C and at this temperature tetragonal-ZrO_2 of Garvie with very

TABLE II Crystalline phases XRD detected and colour evolution with temperature

T(°C)	CE	CEF	CG	CGF	PG	PGF
Raw	M(vs)Q(m), gray	M(s), Q(m) Pr_6O_4(vw) gray	NH_4Cl(m), white	NH_4Cl(m), white	Pr_6O_{11}(vw), gray	Pr_6O_{11}(vw), gray
300	M(vs)Q(m), gray	M(s), Q(m) gray	T(vw), brown	T(vw), brown	A, black	A, black
600	M(vs)Q(m), gray	M(s), Q(m) gray	T(w), brown	T(m), yellow	A, black	P(vw), black
700	M(vs)Q(m), gray	M(s)Q, P(w), white	T(w), yellow	T(m)P(vw), yellow	A, black	P(vw) black
800	M(vs)Q(m), gray	M(s)Q, P(w), white	T(w), yellow	T(m)P(vw), yellow	A, black	P(vw) black
900	M(vs)Q(m), gray	M(s)Q, P(w), white	T(m), yellow	T(m)P(vw), yellow	A, black	T(vw)P(w), gray
1000	M(vs)Q(s), gray	M(s)Q, P(w), white	T(s), yellow	T(s)C, M, P(vw), yellow	T(w), black	T(m)C, M, P(w), white
1100	M(vs)Q(s), gray	M(vs)Q(vw) P(vw) Z(vw), yellow	T, C(vw) M(w), yellow	T(vw)M, P(w) Z(m), intense yellow	T(m), gray	T(m)C, M, P(w), yellow
1200	M(s)Q(m), gray	M, P(vw) Z(vs), intense yellow	T, M, C(vw) Z(vw), yellow	T, P(vw) Z(vs), intense yellow	T(vs), gray	T, P, M(vw), Z(s), intense yellow
1250	M(s)Q(m) Z(vw), gray	M, P(vw) Z(vs), intense yellow	T(vw)M, C(w) Z(m), yellow	T, M, P(vw) Z(vs), intense yellow	T(vs)C(vw) Z(vw), gray	Z(vs), intense yellow
1300	M(s)Q(vw), Z(m), gray	M, P(vw) Z(vs), yellow	T(vw)M, C(w) Z(m), yellow	T, M, P(vw), Z(vs), yellow	T, M(vw)C(w), Z(vs), yellow	Z(vs), yellow

Z ($ZrSiO_4$), T (t-ZrO_2), P ($Na_2Pr_8(SiO_4)_6F_2$), C (Cristobalite), vw (very weak), w (weak), m (medium), s (strong), vs (very strong), Q (Quartz), M (m-ZrO_2).

low crystallite size [21] is crystallized. The colour of the CG sample turns yellowish at 600°C. The addition of NaF to the CGF sample accelerates the crystallization of t-ZrO_2, and it decreases the zircon temperature detection to 1100°C. As in the ceramic samples, $Na_2Pr_8(SiO_4)_6F_2$ crystallizes at 700°C and it remains at 1300°C.

The PG sample remains amorphous and black (due to entrapped C) until 1000°C. At this temperature the t-ZrO_2 of Garvie is crystallized, and the yellow colour and zircon crystallization are delayed until 1300°C.

The addition of NaF in the PGF sample resulted in the crystallization of $Na_2Pr_8(SiO_4)_6F_2$ at 600°C, decreasing both yellow colour appearance temperature and zircon detection to 1000°C and 1200°C respectively.

XRD results in Table II show several facts which must be noted: (a) yellow colour is not associated to NaF addition (CG and PG samples become yellow), but its presence strongly intensifies the colour, (b) in all samples with NaF addition, the $Na_2Pr_8(SiO_4)_6F_2$ phase is detected and remains stable in the overall treatment, except in the PGF sample at 1250–1300°C, where zircon appears as the only XRD detected crystalline phase (solid reaction concluded), (c) the chemical homogeneity of raw powders in PG sample results in a high stability of the amorphous state and in the metastabilization of t-ZrO_2 of Garvie due to the absence of a hetereogeneous nucleation mechanism, but the thermic activation of homogeneous nuclei increases the reactivity of the system and zircon appears as the only crystalline phase detected by XRD in PGF at 1250–1300°C.

3.3. Zircon cell parameters

Measurements of zircon crystallographic parameters by POWCAL and LSQC programmes are shown in Table III. Results indicate that the addition of praseodymium slightly modifies the cell dimensions of zircon. An increase of zircon cell parameters must be expected if praseodymium is incorporated into the zircon lattice (Pauling ratios: Pr^{3+}(1,09 Å), Pr^{4+}(0,92 Å) and Zr^{4+}(0,80 Å)) but the change in cell dimensions might be small depending on the mechanism of incorporation. On the other hand, these parameters neither change in samples fired at 1300°C when a loss of colour intensity is observed. Therefore zircon cell parameters measured indicate the formation of a Pr/zircon solid solution in agreement with previous reported results [5, 8].

TABLE III zircon cell parameters

Sample	T(°C)	$a=b$ (Å)	c (Å)	V (Å^3)
zircon blank		6.594(6)	5.972(7)	259.7(6)
CE	1300	6.601(6)	5.978(6)	260.5(4)
CEF	1250	6.604(1)	5.979(1)	260.8(1)
	1300	6.600(3)	5.980(3)	260.6(2)
CG	1250	6.604(1)	5.983(1)	261.0(1)
	1300	6.600(3)	5.980(3)	260.6(2)
CGF	1250	6.603(2)	5.982(2)	260.8(1)
	1300	6.601(3)	5.981(3)	260.6(2)
PG	1300	6.604(2)	5.980(2)	260.8(1)
PGF	1250	6.608(1)	5.983(1)	261.2(1)
	1300	6.606(2)	5.977(2)	260.8(1)

(Values in parenthesis are the estimated standard deviations in the least significant figure to the left).

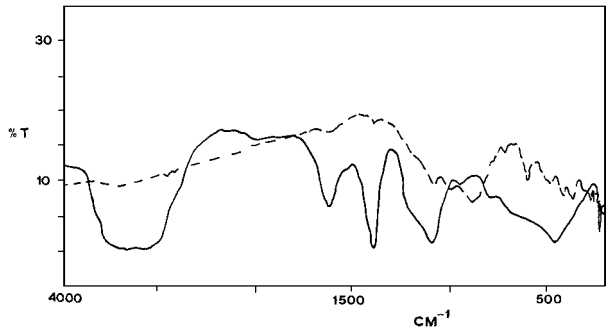

Figure 3 IR spectra of CG sample: raw (——), fired at 1300°C/12 h (- - - -).

3.4. IR (Infrared) spectroscopy

The IR spectra of colloidal sample (CG) are shown in Fig. 3. The IR spectra of gels (CG and PG) contain the 620 cm^{-1} band associated to ZrO_8 group, the 900 cm^{-1} band associated to Si-O^-(O^- meaning non-bridging atom) [22], and a sharp band at 1380 cm^{-1} which can be associated to Zr-O^- terminal groups generated by hydrolisis of $ZrOCl_2.7H_2O$ or zirconium n-propoxide. In all raw samples, bands at 3400 (OH stretching) and 1600 cm^{-1} (H-O-H deformation vibration) are detected due to absorbed water. On the other hand bands at 1200,

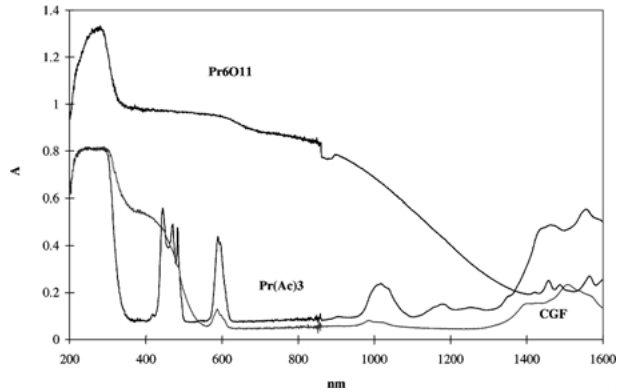

Figure 4 UV-V spectra: CGF (colloidal gel with NaF fired at 1300°C), Pr_6O_{11} (praseodymium oxide), Pr(Ac)3 (Pr(III) acetate).

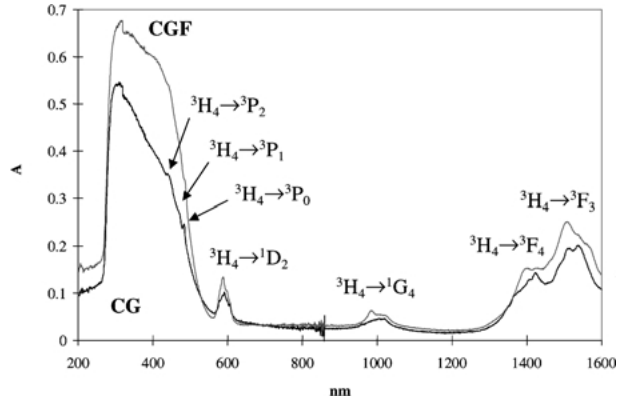

Figure 5 UV-V spectra: CGF (colloidal gel with NaF fired at 1300°C), CG (colloidal gel without NaF fired at 1300°C).

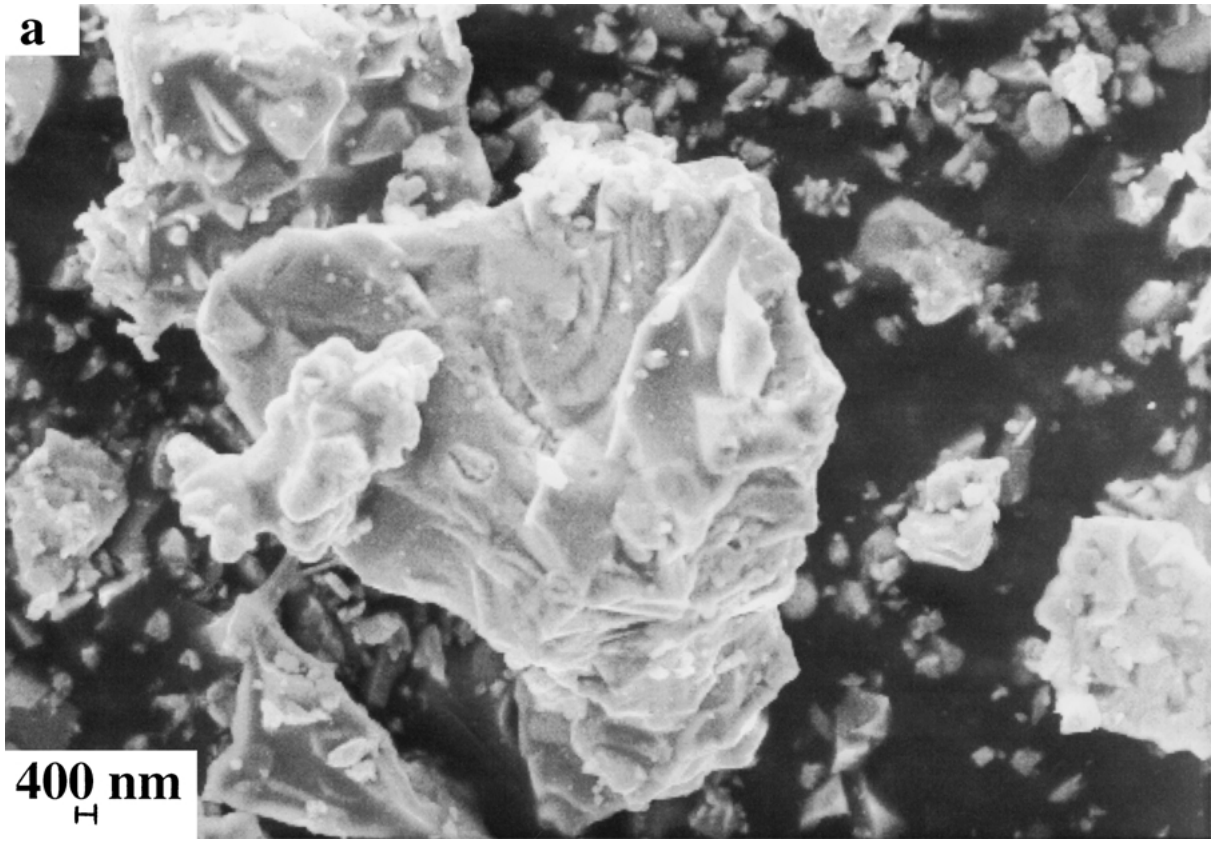

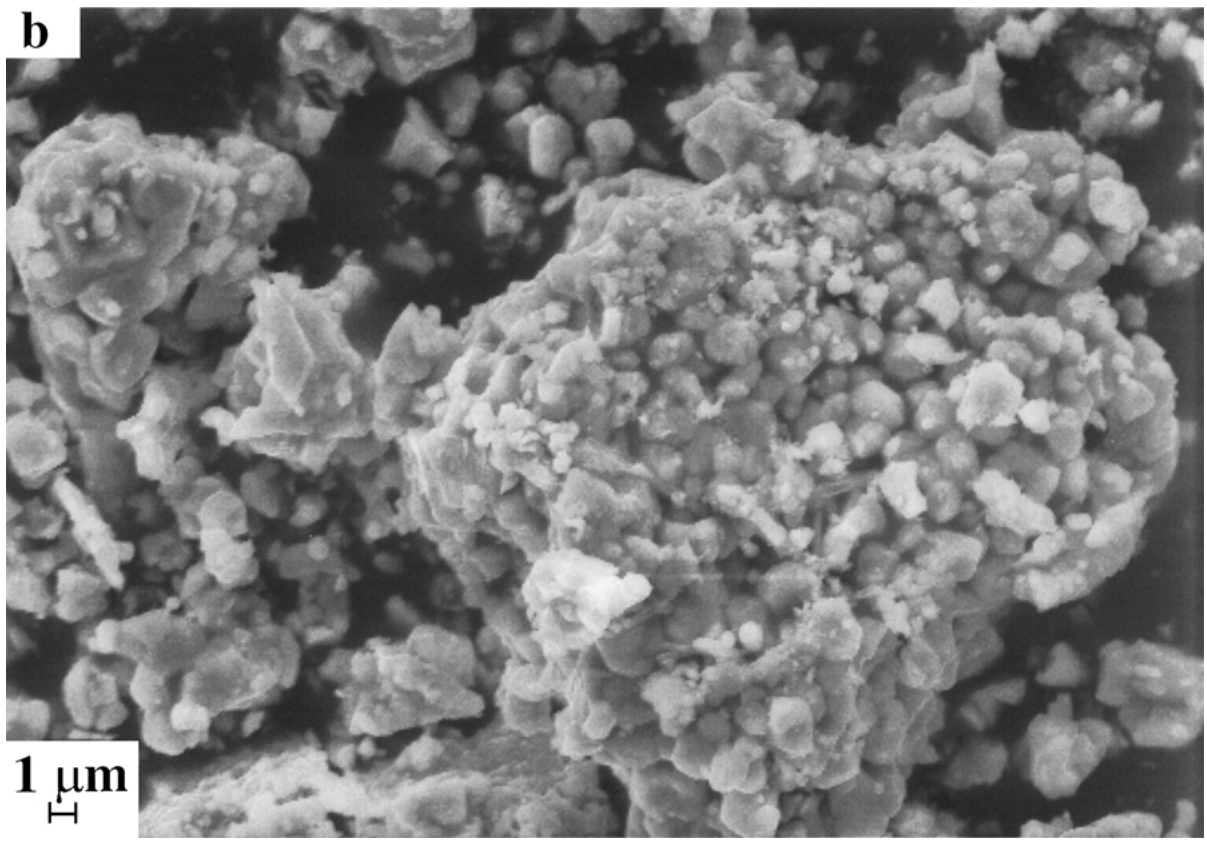

Figure 6 SEM micrographs of samples fired at 1300°C: (a) CEF, (b) CG, (c) CGF, (d) PG. (*Continued*).

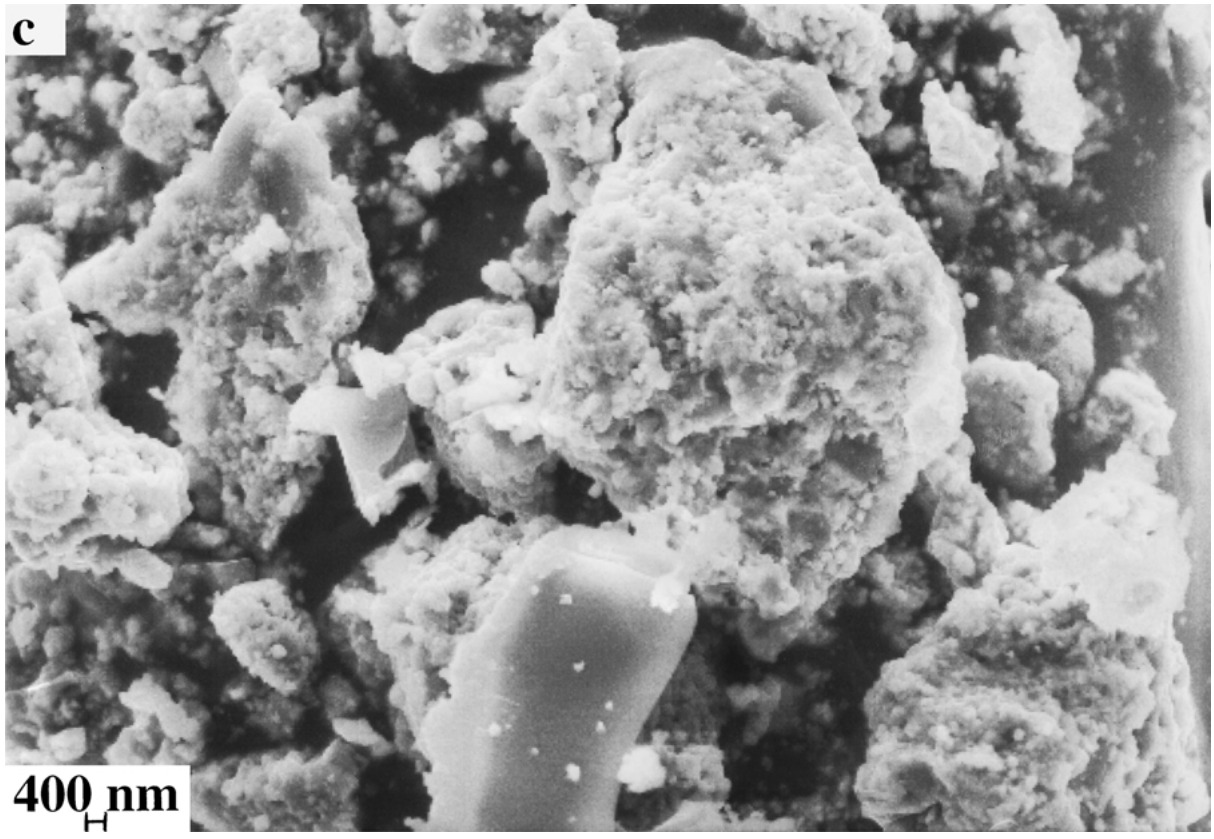

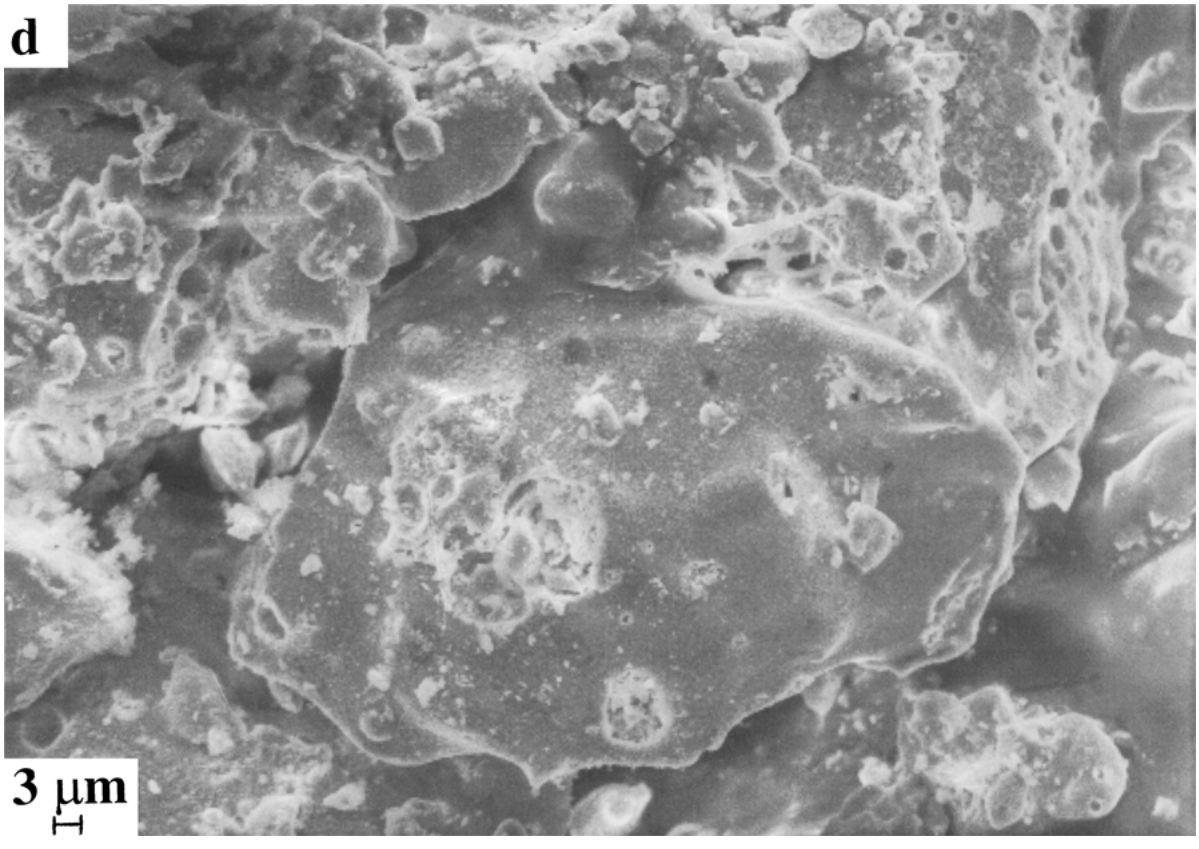

Figure 6 (*Continued*).

1060 cm^{-1} (LO and TO modes of Si-O-Si asymetric bond stretching vibration), 800 cm^{-1} (Si-O-Si symetric band stretching vibration) and 460 cm^{-1} (Si-O-Si bending vibration) are observed. There is not direct evidence of Si-O-Zr bonds in gel samples. In the fired samples, bands at 900, 615, 430, 380 and 300 cm^{-1} associated with zircon [23] are detected.

The presence of the ZrO_8 group in raw gel samples, similar to the dodecahedral group of zirconium in the zircon, explains the higher reactivity of gels. The reactivity is lower than expected because of the metastabilization of the t-ZrO_2 of Garvie of low crystallite size (by 30 nm).

3.5. UV-VIS-NIR characterisation

The valence of the Pr cations was determined from the analysis of the UV-VIS-NIR band spectra of samples fired at 1300°C/12h, which are shown in Fig. 4 along with those obtained for Pr(III) acetate and Pr_6O_{11} (~67% Pr^{4+}) chosen for comparison. As can be seen, our sample (CGF) has similar visible region bands to Pr(III) acetate at 495, 481, 443 and 590–600 nm, due to $^3H_4 \rightarrow {}^3P_\circ, {}^3H_4 \rightarrow {}^3P_1, {}^3H_4 \rightarrow {}^3P_2$ and $^3H_4 \rightarrow {}^1D_2$ transitions. In the near infrared the spectrum of CGF is also similar to Pr(III) acetate with three characteristics bands of Pr(III) cations at 1525, 1423 and 1020 nm associated to $^3H_4 \rightarrow {}^3F_3$, $^3H_4 \rightarrow {}^3F_4$ and $^3H_4 \rightarrow {}^1G_4$ transitions [24, 25] which are shown in Fig. 5. The appearance of the same bands in the UV-V spectrum is consistent with the presence of Pr^{3+} in this pigment.

3.6. CIE-$L^*a^*b^*$ colour measurements

CIE-$L^*a^*b^*$ measurements are summarized in Table IV. As it has been indicated in the XRD results discussion, the yellow colour is associated to the Pr-$ZrSiO_4$ system as well as to Pr-(t-ZrO_2). The intensity of the yellow colour associated to the Pr-$ZrSiO_4$ is higher than in the Pr-(t-ZrO_2). NaF addition strongly increases the yellow intensity (Table IV). This high intensity is related to the high absorbance of these samples in the range between 200–500 nm, but any other difference can not be observed with samples without NaF (Fig. 5).

3.7. Microstructure characterisation (SEM/EDX)

The microstructure of samples fired at 1300°C/12 h is reported in Fig. 6. Zircon appears agglomerated in all samples, but in ceramic and polymeric samples, agglomerates become monolithic (4 μm of average particle size in CEF sample, 40 μm in GP sample). In colloidal gel fired samples, spherical particles (1 μm in CG and 0.4 μm in CGF) form aggregates with an average agglomerate size of 6–20 μm.

The EDX-mapping analysis of the CGF sample fired at 1300°C is shown in Fig. 7. Samples with NaF addition present praseodymium homogeneously dispersed in the material together with high disaggregation of

TABLE IV CIE-$L^*a^*b^*$ measurements

Sample-T(°C)	Pigment system	L^*	a^*	b^*
CG-800	Pr-(t-ZrO_2)	87.3	3.0	26.0
CGF-800	"	90.1	1.0	20.3
CG-900	"	90.3	1.4	24.6
CGF-900	"	90.2	0.3	28.7
CEF-1300	Pr-$ZrSiO_4$	90.6	−6.7	41.4
CG-1300	"	91.0	−3.2	27.7
CGF-1300	"	90.0	−5.6	44.2
PG-1300	"	94.0	−6.6	23.8
PGF-1300	"	90.2	−5.3	43.2

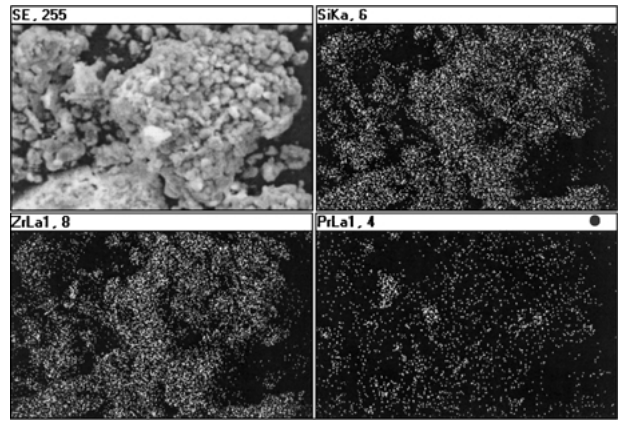

Figure 7 EDX-mapping of CGF sample fired at 1300°C.

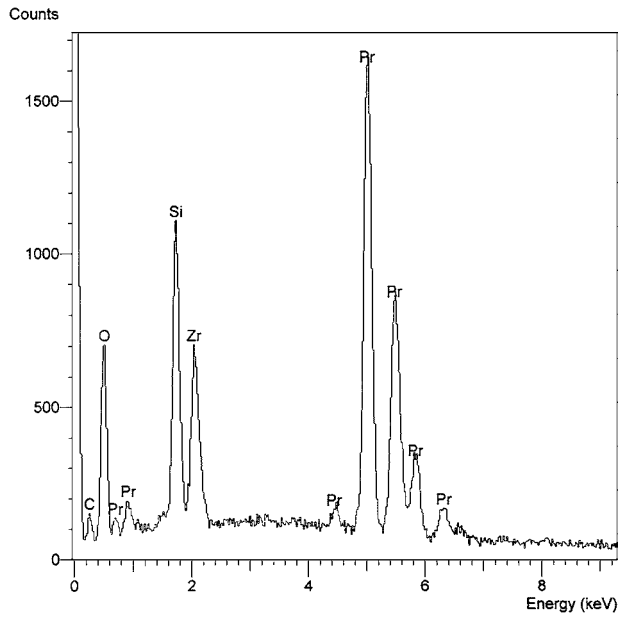

Figure 8 Spot EDX analysis of rich Pr CGF sample fired at 1300°C.

praseodymium (Fig. 7) confirmed by spot analysis of the rich praseodymium particles (Fig. 8). On the contrary, samples without NaF present a homogeneous praseodymium distribution, but the global EDX analysis indicates a lower concentration.

The main results above discussed are in accordance with the possibility of an occlusion mechanism in the pigment: (a) a visual loss of colour is produced at 1300°C and without changing cell parameters of zircon (b) the UV-V spectrum of Pr-$ZrSiO_4$ with NaF addition is similar to sample without NaF: the occluded crystals

present praseodymium ions in similar oxygenated environments, (c) the EDX-mapping analysis indicates the accumulation of the EDX-Pr signal (L^1_α 5.034 KeV) in some particles: this praseodymium hetereogeneity distribution is in agreement with the occlusion mechanism and it can not be explained by a solid solution mechanism. The study of the occluded phase, probably praseodymium oxide (Pr_2O_3 whithout discarding PrO_2 existence) will be the objective for future work.

The role of NaF is to stabilize the $Na_2Pr_8(SiO_4)_6F_2$ phase which retains praseodymium in the reaction media, hence avoiding its volatilization and generating the adequate praseodymium concentration necessary to be able to produce an intense yellow colour.

In order to explain the above results, it is necessary to differentiate the zircon crystallization and the colour production: CE, CG and PG samples are not capable of producing intense yellow colour although a small increase of cell parameters is observed (Pr-zircon solid solution). It is known [24] that by using sol-gel techniques a uniformly dispersed Pr^{3+} content in ceramic matrix is obtained and because of that CG and PG show a soft yellow. The intensity of colour increases in samples with NaF when an adequate synchrony between the zircon crystallization and high amount of praseodymium occlusion occurs.

4. Conclusions

From the above discussion, the following conclusions can be made:

1. The sol-gel synthesis method allows the preparation of yellow Pr-$ZrSiO_4$ pigment at lower temperatures (1100°C in CGF) than the ceramic method. This fact is more relevant in samples without NaF: the reactivity is enhanced when sol-gel methods are employed, both in zircon yield and in yellow colour intensity of samples (not attained by ceramic route without NaF addition).

2. the addition of NaF to the system enhances the reactivity in all samples and it stabilizes $Na_2Pr_8(SiO_4)_6F_2$ crystalline phase from 600–700°C.

3. yellow colour cannot be associated to NaF addition exclusively. UV-V spectra of yellow samples, both with and without NaF addition (CG and PG), are similar but the former has higher absorbances.

4. Pr-$ZrSiO_4$ yellow pigment seems therefore to have a mixed nature: solid solution and encapsulating pigment. This pigment follows an occlusion mechanism when the trivalent praseodymium is present but the cell parameters expansion and homogeneous praseodymium dispersion do not exclude other secondary mechanism of colouring related to the praseodymium solid solution.

Acknowledgments

Authors gratefully acknowledge the financial support of Fundació Caixa Castelló (Project PIA95-10).

References

1. R. EPPLER, *Ceramic Bulletin* **56** (1977) 213.
2. E. KATO and H. TAKASHIMA, *Rep. Gov't. Res. Inst. Ceram. Kyoto* **4** (1956) 147.
3. C. A. SEABRIGHT, US Patent 2,992,123, July 11, 1961.
4. C. A. SEABRIGHT and H. C. DRAKER, *Amer. Ceram. Soc. Bull.* **40** (1961) 1.
5. F. T. BOOTH and G. N. PEEL, *Trans. Brit. Ceram. Soc.* **58** (1959) 532.
6. V. I. MATKOVITCH and P. M. CORBETT, *J. Amer. Ceram. Soc.* **44** (1961) 128.
7. K. SHAW, *Ceramics* **207** (1966) 22.
8. E. H. RAY, T. D. CARNAHAN and R. M. SULLIVAN, *Ceramic Bull.* **40** (1961) 13.
9. BATCHELOR, Meeting of the Pottery Section, Brit. Ceram. Soc., York, 3rd April, 1974.
10. R. A. EPPLER, *J. Amer. Ceram. Soc.* **53** (1970) 8.
11. *Idem.*, *Ind. Eng. Chem. Prod. Res. Dev.* **10** (1971) 352.
12. J. A. HEDVALL, "Solid State Chemistry, Whence, Where and Whiter" (Elsevier, Amsterdam, 1967).
13. H. SCHMALRIZED, *H. Angew. Chem. Int. Ed. Engl.* **2** (1963) 251.
14. G. MONROS, J. CARDA, M. A. TENA, P. ESCRIBANO, M. SALES and J. ALARCÓN, *J. Europ. Ceram. Soc.* **11** (1993) 77.
15. A. C. AIREY and W. ROBERTS, *Ceram. Eng. Sci. Proc.* **8** (1987) 1168.
16. D. R. EPPLER, R. A. EPPLER and CHI-HANG-LI, *ibid.* **13** (1992) 109.
17. M. OCAÑA, A. CABALLERO, A. R. GONZÁLEZ-ELÍPE, P. TARTAJ and C. J. SERNA, *J. Sol. State Chemistry* **139** (1998) 412.
18. M. C. GRAÑANA, J. B. VICENT, M. LLUSAR, M. A. TENA and Y. G. MONRÓS, *Bol. Soc. Cer. Vidr* **39**(2) (2000) 237.
19. POWCAL-LSQC Programmes, Ptt. of Chemistry, Abberdeen University (UK).
20. CIE, Recommendations on Uniform Color Spaces, Color Difference Wquations, Psychometrics Color Terms, Suplement n°2 of CIE Pub., n°15(E1-1.31), Bureau Central de la CIE, Paris, 1978.
21. R. C. GARVIE, R. H. NAHHICK and R. T. PASCOE, *Nature* **258** (1975) 703.
22. M. NOGAMI, *J. Non-Cryst Solids* **69** (1985) 415.
23. G. MONROS, J. CARDA, M. A. TENA, P. ESCRIBANO and J. ALARCÓN, *J. Mater. Sci.* **27** (1992) 351.
24. G. DE, A. LICCIULLI and M. NACUCCHI, *J. Non-Crystalline Solids* **201** (1996) 153.
25. K. WEI, D. P. MACHEWIRTH, J. WENZEL, E. SNITZER and G. H. SIGEL JR., *ibid.* **182** (1995) 257.

Received 23 August 2000
and accepted 29 November 2001